

# 1 Drought conditions disrupt atmospheric carbon uptake 2 in a Mediterranean saline lake

3 Ihab Alfadhel<sup>1,2</sup>, Ignacio Peralta-Maraver<sup>1,2,3\*</sup>, Isabel Reche<sup>1,2,3</sup>, Enrique P.  
4 Sánchez-Cañete<sup>2,4,5</sup>, Sergio Aranda-Barranco<sup>1,4</sup>, Eva Rodríguez-Velasco<sup>1,2,3</sup>,  
5 Andrew S. Kowalski<sup>2,4,5</sup>, Penélope Serrano-Ortiz<sup>1,4\*</sup>.

## 6 7 *Authors adress:*

8 <sup>1</sup>Departamento de Ecología, Facultad de Ciencias, Universidad de Granada, Granada,  
9 Spain.

10 <sup>2</sup>Instituto del Agua, Granada, Universidad de Granada, Spain.

11 <sup>3</sup>Research Unit Modeling Nature (MNat), Universidad de Granada, Granada, Spain.

12 <sup>4</sup>Instituto Interuniversitario de Investigación del Sistema Tierra en Andalucía (IISTA),  
13 Universidad de Granada, Spain

14 <sup>5</sup>Departamento de Física Aplicada, Universidad de Granada, Granada, Spain.

15  
16 \**Correspondence to:* Ignacio Peralta-Maraver ([peraltamaraver@ugr.es](mailto:peraltamaraver@ugr.es)) and Penélope  
17 Serrano-Ortiz ([penelope@go.ugr.es](mailto:penelope@go.ugr.es)).

18  
19 **Abstract:** Saline inland lakes play a key role in the global carbon cycle, acting as  
20 dynamic zones for atmospheric carbon exchange and storage. Given the global decline of  
21 saline lakes and the expected increase of periods of drought in a climate change scenario,  
22 changes in their potential capacity to uptake or emit atmospheric carbon are expected.  
23 Here, we conducted continuous measurements of CO<sub>2</sub> and CH<sub>4</sub> fluxes at the ecosystem  
24 scale in a saline endorheic lake of the Mediterranean region over nearly 2 years. Our focus  
25 was on determining net CO<sub>2</sub> and CH<sub>4</sub> exchanges with the atmosphere under both dry and  
26 flooded conditions, using the eddy covariance (EC) method. We coupled greenhouse gas  
27 flux measurements with water storage and analyzed meteorological variables like air  
28 temperature and radiation, known to influence carbon fluxes in lakes. This extensive data  
29 integration enabled the projection of the net carbon flux over time, accounting for both  
30 dry and wet conditions on an interannual scale. We found that the system acts as a  
31 substantial carbon sink by absorbing atmospheric CO<sub>2</sub> under wet conditions. In years with  
32 prolonged water storage, it is predicted that the lake's CO<sub>2</sub> assimilation capacity can

33 surpass  $-0.7 \text{ kg C m}^2$  annually. Conversely, during extended drought years, a reduction in  
34  $\text{CO}_2$  uptake capacity of more than 80% is expected. Regarding  $\text{CH}_4$ , we measured uptake  
35 rates that exceeded those of well-aerated soils such as forest soils or grasslands, reaching  
36 values of  $-0.2 \mu\text{mol m}^{-2} \text{ s}^{-1}$ . Additionally, we observed that  $\text{CH}_4$  uptake during dry  
37 conditions was nearly double that of wet conditions. However, the absence of continuous  
38 data prevented us from correlating  $\text{CH}_4$  uptake processes with potential environmental  
39 predictors. Our study challenges the widespread notion that wetlands are universally  
40 greenhouse gas emitters, highlighting the significant role that endorheic saline lakes can  
41 play as natural sink of atmospheric carbon. However, our work also underscores the  
42 vulnerability of these ecosystem services in the current climate change scenario, where  
43 drought episodes are expected to become more frequent and intense in the coming years.

44

45 **Keywords:** Intermittent saline lake, eddy covariance, greenhouse gas fluxes, ecosystem  
46 metabolism, Mediterranean shallow lake

47

## 48 1. Introduction

49 Saline inland lakes are diverse and play a crucial role in the global carbon cycle, serving  
50 as dynamic zones for carbon dioxide exchange with the atmosphere (Li et al. 2022; Liao  
51 et al. 2024) and long-term sinks of organic and inorganic carbon (Anderson and Stedmon  
52 2007; Song et al. 2013; Li et al. 2017). In limnology, however, the ecological importance  
53 of these systems has only recently been recognized, despite accounting for approximately  
54 44% of global lake volume and 23% of lake surface area (Messenger et al., 2016). Saline  
55 lakes vary in size from ephemeral ponds to extensive deep-water bodies, such as the  
56 Caspian Sea (Eugster and Hardie, 1978). These lakes are characterized by salinity levels  
57 that exceed 3 parts per thousand and are notably isolated from a direct marine influence  
58 (Williams, 2002; Wang et al., 2018). They are found in endorheic (hydrologically  
59 landlocked) basins across a wide array of climates, spanning cold to warm/hot arid  
60 regions in all continents, including Antarctica (Williams, 2002; Wang et al., 2018). As  
61 terminal points in many hydrological networks, they collect not only significant amounts  
62 of salts but also nutrients and organic and inorganic carbon (Anderson and Stedmon 2007;  
63 Song et al. 2013; Batanero et al. 2017; Li et al. 2017; Liao et al. 2024).

64 Past estimations about the role of saline lakes on global carbon fluxes suggested  
65 that these lakes might function as hotspots for the  $\text{CO}_2$  emission (Duarte et al., 2008).

66 However, more recent works point out that saline lakes have lower partial pressure of  
67 CO<sub>2</sub> than freshwater lakes (Wen et al. 2017) and some systems appear to take up CO<sub>2</sub>  
68 during the winter (Li et al., 2022) or even annually (Yang et al. 2021) due to  
69 physicochemical reactions and increased activity of primary producers. Therefore, more  
70 seasonal studies on CO<sub>2</sub> fluxes in saline lakes are needed to understand the conditions  
71 when these systems behave as sinks or sources of CO<sub>2</sub>. Variations in CO<sub>2</sub> and CH<sub>4</sub> flux  
72 estimates across different studies of water bodies are primarily due to the highly variable  
73 data obtained from discrete sampling (Li et al. 2022) or because of differences in sampling  
74 seasons at the intra-annual scale (Liao et al. 2024). Meanwhile, gathering continuous time  
75 series data on CO<sub>2</sub> and CH<sub>4</sub> sequestration and emission fluxes over years is needed for  
76 accurate assessment of the net carbon balance in inland water systems (Martínez-García  
77 et al. 2024). Nevertheless, long-term, uninterrupted, and direct monitoring of greenhouse  
78 gas flux dynamics at the ecosystem level is relatively scarce in aquatic ecosystems, and  
79 this is particularly true for saline lakes. To the best of our knowledge, only a couple of  
80 studies have reported continuous year-round direct measurements at the ecosystem scale  
81 for CO<sub>2</sub> fluxes (Yang et al. 2021; Li et al. 2022). However, saline lakes' characteristics  
82 differ with latitude (Hammer 1986) and could have very different behaviors regarding  
83 carbon exchanges depending on climate conditions.

84 The carbon hydrochemistry in permanent saline lakes, especially in mountainous  
85 and Arctic latitudes such as the Tibetan Plateau or Svalbard is largely influenced by  
86 surface ice formation (Anderson et al., 2004; Rysgaard et al., 2012, 2013; Wu et al., 2014;  
87 Yan and Zheng, 2015). In contrast, saline lakes in arid and semi-arid endorheic basins,  
88 including Mediterranean climates, are typically shallow, often ephemeral, and/or  
89 hypersaline due to evaporation exceeding precipitation (García et al., 1997; Batanero et  
90 al. 2017; Saccò et al., 2021). The lower depths and higher surface-to-volume ratio, driven  
91 by drought conditions, induce significant physicochemical fluctuations in these saline  
92 inland water bodies, spanning from diurnal to interannual scales (Comin et al. 1990;  
93 García and Niell 1991; García et al. 1997; Batanero et al. 2017). Consequently, the  
94 precipitation regime and subsequent changes in groundwater levels determine the ecology  
95 of saline lakes in arid and semi-arid regions. However, research on the interannual  
96 variability of carbon fluxes in saline lakes affected by seasonal flooding and drought is  
97 lacking. This knowledge gap urgently requires focused research to elucidate the impacts  
98 of climatic variability on the carbon dynamics of these ecosystems, which have been  
99 identified as particularly vulnerable to climate fluctuations (Tweed et al., 2011).

100 Furthermore, recent studies highlight a global decline in lake water storage in most  
101 endorheic basins and in the Sahara, Arabia, and Southern Europe basin in particular  
102 (Wang et al. 2018), a situation expected to worsen with more severe droughts in a climate  
103 change scenario, leading to lower water levels and prolonged desiccation periods  
104 (Wurtsbaugh et al., 2017; Hassani et al., 2020).

105 In this study, we carried out continuous and interannual measurements of CO<sub>2</sub> and  
106 CH<sub>4</sub> fluxes at the ecosystem level in Spain's saline lake Fuente de Piedra using the Eddy  
107 Covariance (EC) method. Serving as a model of a Mediterranean shallow saline lake, it  
108 is characterized by sporadic episodes of water retention but predominantly dry during the  
109 summer. It is worth noting that Fuente de Piedra Lake was designated as a Ramsar site in  
110 1983, ensuring a rich history of monitoring water storage and the various meteorological  
111 drivers of CO<sub>2</sub> and CH<sub>4</sub> fluxes. The objectives of our work are a) to quantify carbon  
112 exchanges during the dry and the flooded conditions, determining its role as a carbon  
113 source or sink, b) to evaluate main drivers promoting carbon exchange behaviors, and  
114 finally c) to use available records of the time series for the main drivers of fluxes to model  
115 the annual net carbon flux of the system in the past. Our research aims to enhance our  
116 understanding of the carbon dynamics and the impacts of climate change on the net carbon  
117 balance in Mediterranean intermittent endorheic lakes.

118

## 119 **2. Material and methods**

### 120 ***Study Site***

121 Fuente de Piedra is a shallow and saline lake located in an endorheic basin in the province  
122 of Málaga, Andalusia, Spain (37.11 N, -4.77 W, elevation 410 m: **Fig 1**). It spans  
123 approximately 17 km<sup>2</sup>, measuring 6.8 km in length and 2.5 km in width, with a maximum  
124 depth of 1.5 meters. We take advantage of Fuente de Piedra Lake's inclusion in the  
125 Ramsar Convention in 1983. This designation ensures a rich history monitoring of water  
126 storage and the meteorological drivers discussed in this article. Such a comprehensive  
127 dataset allows for the back projection of the net carbon flux of the system over time,  
128 incorporating both dry and wet conditions at an interannual scale. This lake is recognized  
129 as a vital habitat within a protected wetland at various levels—regional (as a natural  
130 reserve), European (designated as a special bird protection area), and international  
131 (acknowledged as a Ramsar site)—and offers an exemplary nesting ground for the pink  
132 flamingo (*Phoenicopterus roseus*), largely due to its shallow waters. Among primary

133 producers, diatoms constitute the largest fraction of primary producers of the  
134 phytoplankton all through the year, being dominated by *Hantzschia amphioxys*, *Amphora*  
135 *coffeaiiformis*, *Stauronensis amphioxys*, *Cocconeis placentula*, *Entomoneis* sp. and  
136 several species of *Navicula* and *Nitzschia* sp. (García and Niell, 1993).

137 Salinity levels in the lake vary significantly, ranging from oligosaline (5 ppt) to  
138 hypersaline conditions (> 200 ppt), influenced by the annual hydrological cycle (Batanero  
139 et al. 2017). This cycle is delineated into two distinct phases: a pooling phase during  
140 autumn and winter (December to March), and an evaporative and drought phase spanning  
141 spring and summer (April to November). The lake primarily receives water from  
142 groundwater inflow (Rodríguez- Rodríguez et al. 2006), complemented by contributions  
143 from two streams (**Fig. 1**) and surface runoff from surrounding farmlands. Notably, the  
144 stream entering from the northeast adds nutrients. However, sediment samples distributed  
145 across the lake and analyzed through combustion (Heiri et al., 2001) showed it to be  
146 homogeneous in organic carbon ( $0.21 \pm 0.07$  mg C), nitrogen ( $0.015 \pm 0.004$  mg N) and the  
147 C:N ratio ( $14.4 \pm 2.3$ ).

148

#### 149 ***Field measurements of greenhouse gas fluxes and meteorological drivers.***

150 We employed the eddy covariance method to quantify the exchanges of CO<sub>2</sub>, CH<sub>4</sub>, and  
151 energy (sensible and latent heat) every 30 min from August 2021 to May 2023. Thus, the  
152 eddy covariance system was operated for more than 21 months, including two dry periods  
153 in summer. An open-path eddy covariance (EC) system was strategically positioned atop  
154 a tower, 3.1 meters above ground level, on the western bank of the lake (**Fig.1**). This setup  
155 included two open-path infrared gas analyzers: the LI7500 for CO<sub>2</sub> and water vapor, and  
156 the LI7700 for CH<sub>4</sub> (LICOR Inc., Lincoln, NE, USA). Wind vector components (u, v, w)  
157 and sonic temperature were accurately measured using a sonic anemometer (R.M. Young  
158 81000V, Traverse City, MI, USA). These data were recorded on a data logger (CR1000,  
159 Campbell Scientific, Logan, UT, USA) at a frequency of 10Hz.

160 In addition to gas measurements, we measured a comprehensive suite of  
161 environmental and soil state variables every 10 seconds to capture the conditions over a  
162 representative ground surface area and collected every 30 min average by a data logger  
163 (CR1000, Campbell Scientific, Logan, UT, USA). Air temperature (T<sub>a</sub>) and relative  
164 humidity (RH) were monitored using a thermohygrometer (HMP 45C, Campbell  
165 Scientific, Logan, UT, USA). Net radiation (R<sub>n</sub>) was quantified by a net radiometer (NR  
166 Lite, Kipp and Zonen, Delft, Netherlands). Soil heat flux (G) calculations, including the

167 energy stored in the soil, were facilitated by one heat flux plate (HFP01SC, Hukseflux,  
168 Delft, Netherlands) placed at 8 cm depth, complemented by three pairs of soil temperature  
169 probes (TCAV, Campbell Scientific, Logan, UT, USA) situated at depths of 4 cm and  
170 lateral distances of 3.20 m, 6.34 m, and 8.90 m from the tower.

171 The groundwater level (GWL) was monitored daily using a piezometer situated  
172 within a well in the salt flats, approximately 2 kilometres south of the EC tower and on  
173 the opposite side of the lake (37.1071° N, -4.7631° W; Fig S1). The location of the  
174 piezometer coincides with the central and deepest part of the lake when there is water.  
175 Negative GWL values indicate conditions when the lake is entirely lacking surface water.  
176 Positive values measured by the piezometer were used to determine the lake depth.  
177 Furthermore, data on daily precipitation (PPT), air temperature, and incident solar  
178 radiation (spanning wavelengths from 350 to 1100 nm) were acquired from a  
179 meteorological station located adjacent to Fuente de Piedra Lake, in Sierra Yeguas  
180 (37.1383° N, -4.8358°; 467 m.a.s.l.). The tower setup and instruments were maintained  
181 (mainly cleaning lenses of the open path sensors) every two weeks.

182

### 183 ***Greenhouse gas flux data processing, quality control and partitioning***

184 Half-hourly means (48 measurements per day), variances, and covariances of greenhouse  
185 gas fluxes, adhering to the principles of Reynolds decomposition, were calculated using  
186 the EddyPro® 7.0.7 software (Li-Cor), according to international standards and protocols  
187 (Sabbatini et al., 2018). The data processing protocol encompassed the following steps:  
188 (1) axis rotation for tilt correction using the double rotation method (Wilczak et al., 2001),  
189 (2) turbulent fluctuations were calculated using block averaging method, (3) time lag was  
190 compensated by covariance maximization with default, (4) Webb–Pearman–Leuning  
191 (WPL) correction of air density fluctuation (Webb et al., 1980), (5) despiking and raw  
192 data statistical screening (Vickers and Mahrt, 1997) and (6) spectral corrections of high-  
193 and low-pass filtering effects. Regarding the latter, high-frequency loss due to path  
194 averaging, signal attenuation and sensor separation was compensated according to  
195 Moncrieff et al., (1997), whereas low-frequency loss due to finite time averaging length  
196 and detrending was corrected according to Moncrieff et al. (2004). Quality check flags  
197 were calculated for flux data according to the widely adopted methodology combining  
198 two tests: steady state test and the developed turbulent conditions test. Over the study  
199 period, we only selected high-quality fluxes (flag value =0) measured when the open-path  
200 sensors were totally clean according to their respective Automatic Gain Control (AGC)

201 values (AGC value equal to or above 56 for Open path LI-7500A CO<sub>2</sub> /H<sub>2</sub>O analyzer and  
202 AGC value equal to or higher than 20 for LI-7700).

203 To quantify the sampling area of flux measurements, a footprint model was  
204 estimated using the method by Kljun et al., (2004); **Fig 1**). Data periods when the wind  
205 came from the terrestrial adjacent environment (251° to 59°) were rejected, representing  
206 between 45% and 70% of the available daytime and night-time data respectively during  
207 the dry season (GWL=0), and 30% of the available daytime and night-time data  
208 respectively during the wet seasons (GWL>0). Overall, for the nearly 2 years of  
209 measurements, 18% and 8% of the potential daytime data were of good quality for CO<sub>2</sub>  
210 and CH<sub>4</sub> fluxes respectively. For night-time, the available data were reduced to 10 and  
211 5% respectively. In order to provide additional information regarding the turbulent flux  
212 quality (Moncrieff et al 1997), we calculated the energy balance closure (ratio of the sum  
213 of sensible and latent turbulent fluxes, H + LE, to the net radiation minus soil heat flux,  
214 R<sub>n</sub> - G) using all the available data during the drought period. The obtained value. was  
215 76% (R<sup>2</sup> = 0.64; n = 3117) and is within the range of most the reported FLUXNET sites  
216 (Wilson et al 2022; Stoy et al., 2013)

217

### 218 ***Predicting greenhouse gas fluxes as responses to meteorological drivers***

219 We examine the relationship of CO<sub>2</sub> and CH<sub>4</sub> fluxes in response to groundwater level,  
220 serving as a proxy for long-term water storage, with air temperature as the main factor  
221 regulating respiration in the system, and incident solar radiation modulating the  
222 photosynthetic rate. Since these variables were measured every 24- hours, we processed  
223 half-hourly CO<sub>2</sub> and CH<sub>4</sub> fluxes collected to construct 24-hour integrated values. It is  
224 important to note that gaps in long-term data records are inevitable when using eddy  
225 covariance, primarily due to instrument failure and insufficient turbulence (Falge et al.,  
226 2001; Baldocchi et al., 2003; Aubinet et al., 2012). Additionally, data coverage is often  
227 reduced when wind originates from undesirable sectors, though this does not necessarily  
228 compromise measurement quality (Goloub et al., 2023). Despite these limitations, most  
229 studies derive their primary results from annual or seasonal CO<sub>2</sub> and CH<sub>4</sub> balances using  
230 various gap-filling procedures. In contrast, we exercise greater caution with our limited  
231 data coverage, being very restrictive in quantifying daily fluxes. We selected dates with  
232 over 50% of the anticipated data points, particularly those with more than 25 valid  
233 measurements well-distributed throughout the day, to calculate integrated daily flux.  
234 Before integrating daily flux values, we filled gaps in the half-hourly CO<sub>2</sub> and CH<sub>4</sub> flux

235 data using linear interpolation for missing values. This selection criterion aimed to  
236 accurately represent the daily pattern in flux measurement distribution. Then, a  
237 trapezoidal integration of the values measured every 30 minutes was performed to  
238 calculate the daily flux.

239 To analyze the relationship between integrated daily fluxes and their potential  
240 environmental predictors, we employed a linear regression combined with a forward  
241 model selection technique (Aho et al 2014). This method involved sequentially fitting a  
242 series of regression models, each incorporating different combinations of predictors and  
243 their interactions. The process began with simple models, each containing only one  
244 primary predictor, and gradually increased in complexity to include all possible  
245 interactions among predictors. We then used the Akaike Information Criterion (AIC) to  
246 evaluate and identify the most effective model from the set. The model with the lowest  
247 AIC was selected as the best fit, indicating it provides the most useful balance between  
248 model complexity and explanatory power. After selecting the model, we examined the  
249 influence of the predictors by analyzing the slope  $\beta$  coefficients at a significance level of  
250  $\alpha = 0.05$ , using a 95% confidence interval to determine if these coefficients were  
251 significantly different from zero. Additionally, while ground water level (GWL) was  
252 measured daily, our model selection process also aimed to identify which daily  
253 measurements of air temperature and incident solar radiation (mean, minimum, or  
254 maximum) were the best predictors. This method ensured that the chosen model is robust  
255 and relevant to the ecological scales being studied.

256 Finally, the chosen candidate model for predicting the fluxes in the system was  
257 fitted using available records for the studied drivers, covering the period from 2001 to the  
258 present at Fuente de Piedra Lake. This approach aimed to retrospectively model the fluxes  
259 in the system. Detailed instructions on how to run these analyses are in the R script  
260 available in DRYAD (see details in the *data accessibility statement* section).

261

### 262 **3. Results**

#### 263 *Time series of greenhouse gas emissions and meteorological drivers*

264 At Fuente de Piedra Lake, we observed significant seasonal variations in meteorological  
265 conditions, as illustrated in **Fig 2A**. Air temperature ( $T_a$ ) and incident solar radiation  
266 exhibited consistent trends throughout the study period, with mean daily values of  $17 \pm 7$   
267  $^{\circ}\text{C}$  for  $T_a$  and  $18 \pm 8 \text{ MJ m}^{-2} \text{ d}^{-1}$  for incident solar radiation. In contrast, these two



268 environmental variables generally followed asynchronous patterns with groundwater  
269 level (GWL) and precipitation events, except for a brief peak in precipitation and an  
270 increase in GWL between August and September 2021 (Fig. 2A and B). Particularly  
271 during the summer months (July, August, September), the highest daily air temperature  
272 values coincided with GWLs beneath the surface and a lack of precipitation. Also, during  
273 dry conditions, a salt crust several centimeters thick developed on the sediment (see  
274 Figure 3B). For instance, the minimum  $T_a$  recorded was 2 °C in January 2023  
275 corresponding with a period of frequent precipitation and GWL above the surface.  
276 Conversely, the maximum  $T_a$  of 34 °C occurred in August 2021, during a period when  
277 the GWL was 24 cm below the surface.

278         After the study period, we were able to collect 4,128 measurements for CO<sub>2</sub> fluxes  
279 and 2,425 measurements for CH<sub>4</sub> fluxes, which were relatively well-distributed over the  
280 study period. We observed a strong correspondence between water storage in Fuente de  
281 Piedra Lake and its capacity to assimilate atmospheric CO<sub>2</sub>. The CO<sub>2</sub> flux patterns can be  
282 categorized into two distinct lake states: a flooded lake (groundwater level >0 cm,  
283 indicated from purple to blue colour in **Fig 2C and D**) and a dry lake (groundwater level  
284 <0 cm, shown from orange to yellow colour). During flooding conditions, the lake acted  
285 as a CO<sub>2</sub> sink, with fluxes ranging from 0 to -30  $\mu\text{mol m}^{-2} \text{s}^{-1}$ . The CO<sub>2</sub> assimilation  
286 capacity increases with groundwater level and incident solar radiation, particularly from  
287 January to June.

288         Notably, the flooded conditions in the two years of the study showed marked  
289 differences in groundwater level. In 2022, we recorded the highest CO<sub>2</sub> uptake of 30  $\mu\text{mol}$   
290  $\text{m}^{-2} \text{s}^{-1}$  and an averaged value of -3.11  $\mu\text{mol m}^{-2} \text{s}^{-1}$  during May, when the groundwater  
291 level was at its peak, 40 cm above the surface. This period was also characterized by high  
292 variability in CO<sub>2</sub> flux, occasionally showing peaks of CO<sub>2</sub> outgassing approaching 20  
293  $\mu\text{mol m}^{-2} \text{s}^{-1}$ . The peak CO<sub>2</sub> uptake in 2023 was approximately half of what was observed  
294 in 2022. Although this peak occurred in March rather than May, it followed a similar  
295 trend to the ground water level (GWL), which was also about half of the peak level  
296 observed in 2022 (~20 cm above the surface) resulting in averaged CO<sub>2</sub> uptake values of  
297 -3.66  $\mu\text{mol m}^{-2} \text{s}^{-1}$ . In contrast, under dry conditions, Fuente de Piedra Lake ceases CO<sub>2</sub>  
298 uptake, occasionally transitioning to minor CO<sub>2</sub> emissions. Notice that during extreme  
299 rainfall pulses within dry conditions, when Fuente de Piedra Lake remained relatively dry  
300 with the groundwater level below the surface, we observed notable net CO<sub>2</sub> emissions.  
301 For example, a heavy rainfall event in September 2021 (36 mm day<sup>-1</sup>) resulted in CO<sub>2</sub>

302 emissions reaching up to  $10 \mu\text{mol m}^{-2} \text{s}^{-1}$ , with a high elevation of the groundwater level  
303 above the surface (from -20 to near 20 cm). Also, in October of both 2021 and 2022,  
304 subsequent rainfall events ( $12 \text{ mm day}^{-1}$  and  $22 \text{ mm day}^{-1}$ , respectively) corresponded  
305 with  $\text{CO}_2$  emissions of  $7 \mu\text{mol m}^{-2} \text{s}^{-1}$  and  $5.5 \mu\text{mol m}^{-2} \text{s}^{-1}$ , respectively. In these cases,  
306 emissions occurred under negative GWL conditions.

307 In the case of  $\text{CH}_4$ , the flux was relatively stable throughout the whole study  
308 period, generally acting as a sink, with values fluctuating between  $-0.2$  and  $0.1 \mu\text{mol m}^{-2}$   
309  $\text{s}^{-1}$  and an average of  $-0.05 \mu\text{mol m}^{-2} \text{s}^{-1}$  for the study period (**Fig 2D**). Furthermore, the  
310 measured  $\text{CH}_4$  fluxes did not seem to align clearly with the meteorological variables  
311 examined (**Fig S1**).

312

### 313 *Fluxes of $\text{CO}_2$ and $\text{CH}_4$ at a daily scale*

314 When examining the daily scale during wet conditions, it becomes evident that  $\text{CO}_2$   
315 assimilation predominantly takes place during daylight hours, specifically between 9 a.m.  
316 and 2 p.m. (local time) (**Fig. 3**). It should be noted that the few emission values observed  
317 within this time frame correspond to the emission occurrences described earlier for the  
318 dry season, which promptly followed rainfall events. In the case of dry condition, it is  
319 noteworthy that a salt crust forms over the lake, leading to a near cessation of  $\text{CO}_2$  fluxes.  
320 In the case of  $\text{CH}_4$ , there is also a discernible increase in assimilation fluxes between 9  
321 a.m. and 2 p.m. This observed pattern is consistent in both wet and dry conditions.

322

### 323 *Model predictions of 24-hour integrated flux values in the study system*

324 No evident relationship between  $\text{CH}_4$  flux and the environmental predictors studied was  
325 found during the study period. Additionally, measurements obtained from the EC tower  
326 resulted in a substantial number of gaps in the  $\text{CH}_4$  time series, making it impossible to  
327 establish a predictive model for these fluxes. On the contrary, we were able to adjust a  
328 robust regression model for  $\text{CO}_2$  integrated daily flux. A total of 26 daily integrated  $\text{CO}_2$   
329 flux values were obtained for the sampling period, analyzing those dates when more than  
330 25 valid measurements were available. After AIC model selection routine, the candidate  
331 predictive model for daily integrated  $\text{CO}_2$  flux was determined to include groundwater  
332 level, maximum daily air temperature, and mean incident solar radiation. Additionally,  
333 the model incorporated interactions between groundwater level and maximum daily air  
334 temperature, as well as between groundwater level and incident solar radiation (Summary

335 Table of the model is available in the Supplementary Material). Indeed, the fitted  
336 statistical model has a relatively high explanatory capability (Adjusted  $R^2 = 0.73$ ).

337 The model confirmed a positive effect of groundwater level on enhancing  $CO_2$   
338 assimilation in the system (**Fig 4A**;  $\beta_{GWL} = -0.115$ , 95% CI = -0.214 to -0.016; note that  
339 assimilation corresponds with negative values of the  $CO_2$  flux). While the isolated impact  
340 of air temperature increase on  $CO_2$  assimilation could not be determined ( $\beta_{Ta} = +0.07$ ,  
341 95%CI = -0.053 to +0.192), the model identified an antagonistic interaction between air  
342 temperature and groundwater level ( $\beta_{GWL \times Ta} = +0.010$ , 95%CI = +0.005 to +0.015). As  
343 air temperature increases, the positive effect of GWL on  $CO_2$  assimilation diminishes (**Fig**  
344 **4B**). Conversely, mean daily incident solar radiation was found to promote  $CO_2$   
345 assimilation ( $\beta_{Rad} = -0.12$ , 95%CI = -0.21 to -0.03), with a pronounced synergy between  
346 mean daily incident solar radiation and the presence of water ( $\beta_{GWL \times Rad} = 95\%CI = -$   
347  $0.0116$  to  $-0.003$ ), notably enhancing the capacity for  $CO_2$  assimilation (**Fig 4C**).

348 Using time series data for groundwater level, daily maximum air temperature, and  
349 mean daily incident solar radiation at Fuente de Piedra Lake, we generated retrospective  
350 predictions of  $CO_2$  assimilation capacity in the system dating back to 2001 (**Fig 4D**). The  
351 model predictions closely aligned with the observed values for the study period when  
352 using the time series data for the predictors, supporting the robust predictive ability of our  
353 model (Supplementary Material; **Fig S2**). Our estimates indicate a pronounced fluctuation  
354 in  $CO_2$  assimilation capacity according to hydrological variations. In years with higher  
355 groundwater level and prolonged water storage the model predicted an exceptionally high  
356 capacity for atmospheric  $CO_2$  assimilation of the lake, with annual values surpassing  $0.7$   
357  $Kg\ C\ m^{-2}\ year^{-1}$  (e.g., in 2011, 2012, 2014, 2020). In contrast, during years marked by  
358 extended droughts, a substantial reduction in  $CO_2$  assimilation capacity was modeled,  
359 with predicted reductions exceeding 80% compared to wetter years (Fig. 4D). These  
360 drought periods, resulted in a reduction of the assimilation capacity to less than a third of  
361 the levels recorded in wet years (e.g., from 2006 to 2010).

362

#### 363 **4. Discussion**

364 In agreement with previous research on permanent saline lakes of the Tibetan plateau (Li  
365 et al. 2022), we demonstrate that a model Mediterranean shallow saline lake serves as a  
366 substantial carbon sink, absorbing atmospheric  $CO_2$  when flooded. In particularly wet  
367 years, expected uptake values can exceed  $-1.2\ kg\ C\ m^{-2}\ year^{-1}$ . Sporadic instances were

368 also observed where the system acted as a CO<sub>2</sub> emitter, resulting from rewetting events  
369 that followed rainfall during dry conditions. Conversely, CO<sub>2</sub> uptake ceases during dry  
370 conditions, reducing the system's capacity in dry years to below -0.2 kg C m<sup>-2</sup> year<sup>-1</sup>.  
371 Longitudinal time series analysis reveals that prolonged droughts indeed hinder the ability  
372 of the system to assimilate atmospheric CO<sub>2</sub> due to the lack of water, but we also observed  
373 that an increase in air temperature during wet conditions moderates the CO<sub>2</sub> net  
374 assimilation capacity, a process likely related to the reduction of gas water solubility with  
375 temperature. This underscores the pronounced impact of seasonal and interannual  
376 variability, ultimately dictated by drought and rainfall patterns, on the ability of the  
377 studied system to sequester atmospheric carbon. Moreover, this pattern also displayed  
378 considerable variability at the daily scale, closely correlating with fluctuations in incident  
379 solar radiation over daily cycles. In this regard, the CO<sub>2</sub> assimilation capacity of the  
380 system peaked during those hours of maximum incident solar radiation. While  
381 measurement of CO<sub>2</sub> (and CH<sub>4</sub>) fluxes at multiple scales is challenging and requires  
382 specialized equipment (i.e. eddy covariance sensors), our research proposes an alternative  
383 proxy. By integrating data from environmental predictors at various scales we have been  
384 able to reconstruct the behavior of CO<sub>2</sub> exchanges between Fuente de Piedra Lake and  
385 the atmosphere. In essence, we estimate CO<sub>2</sub> flux through the continuous measuring of  
386 accessible environmental variables, namely, the amount of water, air temperature, and  
387 incident solar radiation.

388 In shallow, well-mixed, and oxygenated systems like Fuente de Piedra Lake, the  
389 photosynthetic capacity of the phytoplankton community is closely linked to the water  
390 column height (i.e. groundwater level; Batanero et al. 2017), promoting CO<sub>2</sub> assimilation  
391 as the extent of the habitat for these communities expands (Wetzel, 2001). Related to the  
392 aforementioned, a significant synergy exists between water storage in the ecosystem and  
393 incident radiation, serving as a proxy for the photosynthetically active radiation upon  
394 which photosynthesis depends. This interaction occurs on both a daily scale, associated  
395 with variations in light intensity following day-night cycles, and an annual seasonal scale,  
396 largely determined by changes in daylight hours throughout the year. Notably, during the  
397 night, the net exchange of CO<sub>2</sub> between the water and the atmosphere in Fuente de Piedra  
398 Lake is negligible. This could be attributed to the absence of photosynthesis during  
399 nighttime. Additionally, the high salinity inherent to these environments constrains  
400 methanogenesis, which is the least energy-efficient carbon mineralization process in the  
401 redox sequence (reviewed in Soued et al., 2024). Considering the above, it appears to

402 offer a plausible explanation for why microbial respiration does not surpass inorganic  
403 carbon assimilation through photosynthesis in systems like Fuente de Piedra Lake during  
404 wet conditions, despite the high content of dissolved organic carbon ranging between  
405 1.00 and 13.59 mmol C L<sup>-1</sup> (Batanero et al., 2017).

406         What is more, despite the limited CH<sub>4</sub> flux data, our results position Fuente de  
407 Piedra Lake as a CH<sub>4</sub> sink. Rough estimates determined that Fuente de Piedra could take  
408 up on average 1.83 mg C m<sup>-2</sup> day<sup>-1</sup> and 3.70 mg C m<sup>-2</sup> day<sup>-1</sup> during wet and the dry  
409 conditions respectively (Supplementary Material; **Fig S3**). Such values are even higher  
410 than those measured in typical well aerated soils as in forests or grasslands, with average  
411 rates of 0.4-1.26 mg C m<sup>-2</sup> day<sup>-1</sup> (Murguia-Flores et al., 2021; Perez-Quezada et al., 2021).  
412 Twice the value of uptake during dry conditions compared to wet ones appear to be  
413 consistent with some proposed mechanisms promoting CH<sub>4</sub> reduction according to the  
414 existing literature, since the increase of temperature together with gas diffusivity due to  
415 loss of water, may increase methane oxydation in a similar way to terrestrial ecosystems  
416 (Chen et al., 2010; Rafalska et al 2023). However, caution is needed when interpreting  
417 our results, as the dynamics of methane fluxes could become very complex in an  
418 intermittent system like Fuente de Piedra. On the one hand, just as methanogenic activity  
419 is inhibited by salinity (Herbert et al., 2015), methanotrophic activity has also been  
420 observed to be significantly reduced by salinity in terrestrial systems (Ho et al., 2018).  
421 However, methane oxydation processes associated with aquatic prokaryotes may be more  
422 resistant to salinity (Khmelenina et al., 2010; Deng et al. 2017), especially if the variation  
423 is gradual (Osudar et al., 2017). Thus, further measurements and analysis are needed to  
424 estimate the role of methane oxydation and the relevance of saline intermitent lakes as  
425 CH<sub>4</sub> sinks in a climate change scenario.

426         Drought conditions are accompanied by an increase in air temperature, with the  
427 high air temperatures recorded immediately before the system completely dries out. We  
428 have found that this rise in air temperature leads to a reduction of the system's capacity  
429 to assimilate CO<sub>2</sub>, even during wet conditions. A direct consequence of climatic warming  
430 is the reduction of gas solubility accentuated in saline wetlands (Batanero et al. 2022). In  
431 addition, an increase in temperature can enhance microbial metabolic rates and therefore,  
432 biomass-specific CO<sub>2</sub> production (Smith et al. 2019). Given that endorheic saline lakes  
433 are fueled by significant amounts of organic matter (Li et al., 2017; Batanero et al., 2017;  
434 Song et al., 2013), it is unsurprising that warming leads to a decrease in net primary  
435 production in the system as a result of enhanced microbial respiration, and consequently,

436 a reduction in CO<sub>2</sub> assimilation capacity. In addition, carbon emissions in inland waters  
437 could increase with warming, independently of organic carbon inputs, simply because the  
438 apparent activation energy is predicted to be higher for respiration than photosynthesis  
439 (Yvon-Durocher et al. 2010; Yvon-Durocher et al. 2012). Finally, it has been recognized  
440 that photosynthesis is often the first process to be affected by environmental stressors,  
441 with photosynthetic capacity diminishing prior to other cellular functions (Feller, 2016;  
442 Cardona et al., 2018). Specifically, carbon assimilation through the Calvin–Benson cycle  
443 exhibits particular vulnerability to both drought and elevated temperatures, occurring  
444 even when photosynthetic electron transport continues to operate effectively (Sharkey,  
445 2005). On the whole, we show the profound synergy between global warming and  
446 intensifying drought severity and frequency, disrupting the CO<sub>2</sub> assimilation capacity of  
447 Mediterranean saline lakes and leading to negative feedback loops.

448 While the desiccation of saline lakes is not novel, with researchers highlighting  
449 the concerning increase in dry periods within many of these ecosystems over recent  
450 decades (Williams 1993; Gross 2017; Wurtsbaugh et al. 2017; Wang et al. 2018), our  
451 study underscores the significant implications this trend has for the ecosystem services  
452 they support. Our retrospective predictions show that in wet years, the system could  
453 exhibit a high CO<sub>2</sub> assimilation rate. For instance, between 2010 and 2015, we estimated  
454 that Fuente de Piedra Lake had an average assimilation rate of 0.83 (SD = ±0.27) kg C m<sup>-2</sup>  
455 year<sup>-1</sup>, within the same range as the net assimilation observed in evergreen or deciduous  
456 forest systems worldwide (Pastorello et al., 2020) and marine salt marshes (Mayen et al.  
457 2024). Considering the 13.6 km<sup>2</sup> area of Fuente de Piedra and assuming a constant flux  
458 across the lake surface when flooded, we could estimate around 11 tons of carbon  
459 sequestered during a wet and fully flooded year. Although this upscaling exercise is crude,  
460 it highlights that Mediterranean shallow saline lakes could be a substantial carbon sink  
461 and underline the potential keeping them inundated with water during their conservation  
462 policies. Therefore, further studies across different Mediterranean shallow saline lakes  
463 are necessary to refine these estimates and enhance our understanding of their role in the  
464 global scale carbon budget.

465

## 466 **5. Conclusion**

467 Our result challenges the generalised belief that inland waters primarily act as sources  
468 of greenhouse gases (Raymond et al. 2013). Conversely, the system undergoes significant

469 reductions in its annual atmospheric CO<sub>2</sub> sequestration capacity during dry conditions.  
470 For instance, under severe drought conditions as observed in Fuente de Piedra from 2005  
471 to 2009, the annual CO<sub>2</sub> sequestration is estimated to have fallen to less than a quarter of  
472 what was observed in more humid conditions. Climate change projections, including even  
473 the most optimistic scenarios, forecast an increase in both the frequency and duration of  
474 heatwaves and droughts in the coming years (Trenberth 2011, Perkins-Kirkpatrick 2020).  
475 This implies that saline lake ecosystems in arid and semi-arid endorheic basins will  
476 remain dry for longer periods, or may even vanish, resulting in the loss of a significant  
477 carbon sequestration pathway. Importantly, the disappearance of saline lakes due to water  
478 scarcity has been largely attributed to anthropogenic water overuse (i.e., agriculture)  
479 rather than to macroclimatic phenomena (Wurtsbaugh et al. 2017). This seems to be the  
480 case of Fuente de Piedra Lake, as the catchment area is dominated by agricultural land.  
481 Thus, a proper water system management during drought conditions seems to be the most  
482 plausible solution to preserve the ecosystem services provided by Mediterranean saline  
483 lakes.

484

#### 485 **Author contribution**

486 PS-O and IR conceived the study; all authors contributed to the installation and  
487 maintenance of the eddy covariance tower; IA led the fieldwork and the processing of the  
488 samples with the help of the rest of the authors; IP-M carried out the analyses and the  
489 preparation of the results; IA, IP-M, and PS-O conducted the preparation of the first draft  
490 of the work; all authors participated in the drafting of the final draft.

491

#### 492 **Data accessibility statement**

493 The R script used to conduct the data analysis and the datasets are available at the Dryad  
494 Digital Repository:

495 <https://datadryad.org/stash/share/qEpPRJopVR132UuszL3bnaxoZh07ADL0E5LpVL6xC>

496 SZA

497

#### 498 **Acknowledgements**

499 We thank the logistic support and groundwater level data provided by the curator of the  
500 Natural Reserve of Laguna de Fuente de Piedra África Lupión Sánchez. Author also  
501 acknowledge the review provided by the anonymous reviewers.

502

503 **Financial support**

504 This work was partially support by the projects PID2020-117825GB-C21 and PID2020-  
505 117825GB-C22 funded by MCIN/AEI/10.13039/501100011033, LifeWatch-2019-10-  
506 UGR-01 and LifeWatch-2019-09-CSIC-13 funded by the MCIN through the FEDER  
507 funds from the Spanish Pluriregional Operational Program 2014-2020 (POPE),  
508 LifeWatch-ERIC action line and project BAGAMET (P20\_00016) funded by the  
509 Counseling of Economy, Innovation, Science and Employment from the Government of  
510 Andalucía, including European Union ERDF funds. I.P.-M. developed his research as  
511 part of the eWARM project, supported by the Marie Skłodowska-Curie postdoctoral  
512 fellowship 2022 (project number 101110111).

513

514 **Competing interests**

515 The authors declare that they have no conflict of interest.

516

517 **References**

518 Aho, K., Derryberry, D., and Peterson, T: Model selection for ecologists: the worldviews  
519 of AIC and BIC. *Ecology*, 95(3), 631-636, <https://doi.org/10.1890/13-1452.1> ,  
520 2014.

521 Anderson, L. G., Falck, E., Jones, E. P., Jutterström, S., and Swift, J. H: Enhanced uptake  
522 of atmospheric CO<sub>2</sub> during freezing of seawater: A field study in Storfjorden,  
523 Svalbard. *J. Geophys. Res. Oceans*, 109(C6)  
524 <https://doi.org/10.1029/2003JC002120>, 2024.

525 Anderson, N. J., and Stedmon, C. A: The effect of evapoconcentration on dissolved  
526 organic carbon concentration and quality in lakes of SW Greenland. *Freshwater*  
527 *Biology*, 52(2), 280-289, <https://doi.org/10.1111/j.1365-2427.2006.01688.x> ,  
528 2007.

529 Aubinet, M., Vesala, T., and Papale, D. Eddy covariance: A practical guide to  
530 measurement and data analysis. London, UK Springer, 2012.

531 Baldocchi, D. D. Assessing the eddy covariance technique for evaluating carbon dioxide  
532 exchange rates of ecosystems: past, present and future. *Glob. Chan. Biol.* 9(4),  
533 479-492, <https://doi.org/10.1046/j.1365-2486.2003.00629.x> , 2003.

534 Batanero, G. L., León-Palmero, E., Li, L., Green, A. J., Rendón-Martos, M., Suttle, C.  
535 A., and Reche, I. Flamingos and drought as drivers of nutrients and microbial



536 dynamics in a saline lake. *Scientific Reports*, 7(1), 12173,  
537 <https://doi.org/10.1038/s41598-017-12462-9> , 2017.

538 Batanero, G. L., Green, A. J., Amat, J. A., Vittecoq, M., Suttle, C. A., and Reche, I.  
539 Patterns of microbial abundance and heterotrophic activity along nitrogen and  
540 salinity gradients in coastal wetlands. *Aquatic Sciences*, 84, 22,  
541 <https://doi.org/10.1007/s00027-022-00855-6>, 2022.

542 Cardona, T., Shao, S., and Nixon, P. J: Enhancing photosynthesis in plants: the light  
543 reactions. *Essays in biochemistry*, 62(1), 85-94,  
544 <https://doi.org/10.1042/EBC20170015> , 2018.

545 Chen, W., Wolf, B., Zheng, X., Yao, Z., Butterbach-bahl, K. L. A. U. S., Brueggemann,  
546 N., ... and Han, X: Annual methane uptake by temperate semiarid steppes as  
547 regulated by stocking rates, aboveground plant biomass and topsoil air  
548 permeability. *Glob. Change Biol.*, 17(9), 2803-2816.  
549 <https://doi.org/10.1111/j.1365-2486.2011.02444.x> , 2011.

550 Comín, F. A., Julia, R., Comin, M. P., and Plana, F: Hydrogeochemistry of Lake  
551 Gallocanta (Aragón, NE Spain). In *Saline Lakes: Proceedings of the Fourth*  
552 *International Symposium on Athalassic (inland) Saline Lakes*, held at Banyoles,  
553 Spain, May 1988 (pp 51-66). Springer Netherlands, 1990

554 Deng, Y., Liu, Y., Dumont, M., and Conrad, R. Salinity affects the composition of the  
555 aerobic methanotroph community in alkaline lake sediments from the Tibetan  
556 Plateau. *Microb. Ecol.*, 73, 101-110, <https://doi.org/10.1007/s00248-016-0879-5> ,  
557 2017.

558 Duarte, C. M., Prairie, Y. T., Montes, C., Cole, J. J., Striegl, R., Melack, J., and Downing,  
559 J. A: CO<sub>2</sub> emissions from saline lakes: A global estimate of a surprisingly large  
560 flux. *J. Geophys. Res. G: Biogeosciences*, 113(G4),  
561 <https://doi.org/10.1029/2007JG000637> , 2008.

562 Eugster, H. P., and Hardie, L. A. (1978). *Saline lakes*. In *Lakes: chemistry, geology,*  
563 *physics* (pp. 237-293). New York, NY: Springer New York.

564 Falge, E., Baldocchi, D., Olson, R., Anthoni, P., Aubinet, M., Bernhofer, C., ... & Wofsy,  
565 S. Gap filling strategies for long term energy flux data sets. *Agric. For. Meteorol.*  
566 107(1), 71-77, [https://doi.org/10.1016/S0168-1923\(00\)00235-5](https://doi.org/10.1016/S0168-1923(00)00235-5) , 2001.

567 Feller, U: Drought stress and carbon assimilation in a warming climate: Reversible and  
568 irreversible impacts. *J. Plant Physiol.*, 203, 84-94,  
569 <https://doi.org/10.1016/j.jplph.2016.04.002> , 2016.

- 570 García, C. M., García-Ruiz, R., Rendón, M., Niell, F. X., and Lucena, J: Hydrological  
571 cycle and interannual variability of the aquatic community in a temporary saline  
572 lake (Fuente de Piedra, Southern Spain). *Hydrobiologia*, 345, 131-141,  
573 <https://doi.org/10.1023/A:1002983723725> , 1997.
- 574 García, C. M., and Niell, F. X: Burrowing beetles of the genus *Bledius* (Staphylinidae) as  
575 agents of bioturbation in the emergent areas and shores of an athalassic inland lake  
576 (Fuente de Piedra, southern of Spain). *Hydrobiologia*, 215, 163-173,  
577 <https://doi.org/10.1007/BF00014719> , 1991.
- 578 García, C. M., and Niell, F. X: Seasonal change in a saline temporary lake (Fuente de  
579 Piedra, southern Spain). *Hydrobiologia*, 267(1), 211-223,  
580 <https://doi.org/10.1007/BF00018803> ,1993.
- 581 Golub, M., Koupaei-Abyazani, N., Vesala, T., Mammarella, I., Ojala, A., Bohrer, G., et  
582 al. Diel, seasonal, and inter-annual variation in carbon dioxide effluxes from lakes  
583 and reservoirs. *Environ. Res. Lett.* 18(3), 034046, [https://doi.org/10.1088/1748-](https://doi.org/10.1088/1748-9326/acb834)  
584 [9326/acb834](https://doi.org/10.1088/1748-9326/acb834) , 2023.
- 585 Guerrero, M. C., and Wit, R. d: Microbial mats in the inland saline lakes of Spain.  
586 *Limnetica*, 8, 197–204, 1992.
- 587 Hammer, U. T: Saline lake ecosystems of the world. Springer Science and Business  
588 Media, 1986.
- 589 Hardie, L. A., Smoot, J. P., and Eugster, H. P: Saline lakes and their deposits: a  
590 sedimentological approach. *Modern and ancient lake sediments*, 7-41, 1978.
- 591 Hassani, A., Azapagic, A., D'Odorico, P., Keshmiri, A., and Shokri, N: Desiccation crisis  
592 of saline lakes: A new decision-support framework for building resilience to  
593 climate change. *Sci. Total Environ.*, 703, 134718,  
594 <https://doi.org/10.1016/j.scitotenv.2019.134718> , 2020.
- 595 Heiri, O., Lotter, A. F., and Lemcke, G.: Loss on ignition as a method for estimating  
596 organic and carbonate content in sediments: reproducibility and comparability of  
597 results. *J. Paleolimnol.*, 25, 101-110, <https://doi.org/10.1023/A:1008119611481> ,  
598 2001.
- 599 Khmelenina, V. N., Shchukin, V. N., Reshetnikov, A. S., Mustakhimov, I. I., Suzina, N.  
600 E., Eshinimaev, B. T., and Trotsenko, Y. A.: Structural and functional features of  
601 methanotrophs from hypersaline and alkaline lakes. *Microbiology*, 79, 472-482,  
602 <https://doi.org/10.1134/S0026261710040090>, 2010.

603 Kljun, N., Calanca, P., Rotach, M. W., and Schmid, H. P.: A simple parameterisation for  
604 flux footprint predictions. *Bound-Lay Meteorol.*, 112(3), 503–523,  
605 <https://doi.org/10.1023/B:BOUN.0000030653.71031.96> , 2004.

606 Ho, A., Mo, Y., Lee, H. J., Sauheitl, L., Jia, Z., and Horn, M. A. Effect of salt stress on  
607 aerobic methane oxidation and associated methanotrophs; a microcosm study of a  
608 natural community from a non-saline environment. *Soil Biol. Biochem.*, 125, 210-  
609 214, <https://doi.org/10.1016/j.soilbio.2018.07.013> , 2018.

610 Li, Y., Zhang, C., Wang, N., Han, Q., Zhang, X., Liu, Y., Xu, L. and Ye, W: Substantial  
611 inorganic carbon sink in closed drainage basins globally. *Nature Geosci.*, 10(7),  
612 501-506, <https://doi.org/10.1038/ngeo2972> ,2017.

613 Li, X. Y., Shi, F. Z., Ma, Y. J., Zhao, S. J., and Wei, J. Q: Significant winter CO<sub>2</sub> uptake  
614 by saline lakes on the Qinghai-Tibet Plateau. *Glob. Change Biol.*, 28(6), 2041–  
615 2052, <https://doi.org/10.1111/gcb.16054> , 2022.

616 Liao, Y., Xiao, Q., Li, Y., Yang, C., Li, J., and Duan, H: Salinity is an important factor in  
617 carbon emissions from an inland lake in arid region. *Sci. Total Environ.*, 906,  
618 167721, <https://doi.org/10.1016/j.scitotenv.2023.167721> , 2024.

619 Martínez-García, A., Peralta-Maraver, I., Rodríguez-Velasco, E., Batanero, G.L., García-  
620 Alguacil, M., Picazo, F., Calvo, J., Morales-Baquero, R., Rueda, F.J., Reche, R:  
621 Particulate organic carbon sedimentation triggers lagged methane emissions in a  
622 eutrophic reservoir. *Limnol. Oceanogr. Lett.*, <https://doi.org/10.1002/lol2.10379> ,  
623 2024.

624 Messenger, M. L., Lehner, B., Grill, G., Nedeva, I., and Schmitt, O: Estimating the volume  
625 and age of water stored in global lakes using a geo-statistical approach. *Nature*  
626 *comm.*, 7(1), 13603, <https://doi.org/10.1038/ncomms13603>, 2016.

627 Moncrieff, J. B., Massheder, J. M., de Bruin, H., Elbers, J., Friborg, T., Heusinkveld, B.,  
628 Kabat, P., Scott, S., Soegaard, H., and Verhoef, A.: A system to measure surface  
629 fluxes of momentum, sensible heat, water vapour and carbon dioxide. *J. Hydrol.*,  
630 188–189, 589–611, [https://doi.org/10.1016/S0022-1694\(96\)03194-0](https://doi.org/10.1016/S0022-1694(96)03194-0) ,1997.

631 Moncrieff, J., Clement, R., Finnigan, J., and Meyers, T: Averaging, Detrending, and  
632 Filtering of Eddy Covariance Time Series. In *Handbook of Micrometeorology*  
633 (pp. 7–31), 2004.

634 Murguía-Flores, F., Ganesan, A. L., Arndt, S., and Hornibrook, E. R.: Global uptake of  
635 atmospheric methane by soil from 1900 to 2100. *Global Biogeochem. Cycles*,  
636 35(7), e2020GB006774, <https://doi.org/10.1029/2020GB006774> , 2021.

637 Osudar, R., Klings, K. W., Wagner, D., and Bussmann, I.: Effect of salinity on microbial  
638 methane oxidation in freshwater and marine environments. *Aquatic Microb. Ecol.*,  
639 80(2), 181-192, <https://doi.org/10.3354/ame01845> , 2017.

640 Pastorello, G., Trotta, C., Canfora, E., Chu, H., Christianson, D., Cheah, Y. W., ... & Law,  
641 B.: The FLUXNET2015 dataset and the ONEFlux processing pipeline for eddy  
642 covariance data. *Sci. Data*, 7, 225, <https://doi.org/10.1038/s41597-020-0534-3>,  
643 2020.

644 Perez-Quezada, J. F., Urrutia, P., Olivares-Rojas, J., Meijide, A., Sánchez-Cañete, E. P.,  
645 and Gaxiola, A.: Long term effects of fire on the soil greenhouse gas balance of  
646 an old-growth temperate rainforest. *Sci. Total Environ.*, 755, 142442,  
647 <https://doi.org/10.1016/j.scitotenv.2020.142442> , 2021.

648 Perkins-Kirkpatrick, S. E., and Lewis, S. C.: Increasing trends in regional heatwaves.  
649 *Nature comm.*, 11(1), 3357, <https://doi.org/10.1038/s41467-020-16970-7> , 2020.

650 Rafalska, A., Walkiewicz, A., Osborne, B., Klumpp, K., and Bieganowski, A.: Variation  
651 in methane uptake by grassland soils in the context of climate change—A review  
652 of effects and mechanisms. *Sci. Total Environ.*, 871, 162127,  
653 <https://doi.org/10.1016/j.scitotenv.2023.162127> , 2023.

654 Raymond, P. A., Hartmann, J., Lauerwald, R., Sobek, S., McDonald, C., Hoover, M., ...  
655 and Guth, P.: Global carbon dioxide emissions from inland waters. *Nature*,  
656 503(7476), 355-359, <https://doi.org/10.1038/nature12760> , 2013.

657 Rodríguez- Rodríguez, M., Benavente, J. and Moral, F.: High density ground-water flow,  
658 major-ion chemistry and field experiments in a closed basin: Fuente de Piedra  
659 Playa Lake (Spain). *American J. Environ. Sciences*. 1, 164–171, 2006.

660 Rysgaard, S., Glud, R. N., Lennert, K., Cooper, M., Halden, N., Leakey, R. J. G., and  
661 Barber, D.: Ikaite crystals in melting sea ice—implications for pCO<sub>2</sub> and pH levels  
662 in Arctic surface waters. *The Cryosphere*, 6(4), 901–908,  
663 <https://doi.org/10.5194/tc-6-901-2012> , 2012.

664 Rysgaard, S., Søgaard, D. H., Cooper, M., Pućko, M., Lennert, K., Papakyriakou, T. N.,  
665 and Barber, D.: Ikaite crystal distribution in Arctic winter sea ice and implications  
666 for CO<sub>2</sub> system dynamics. *The Cryosphere*, 7(2), 707–718,  
667 <https://doi.org/10.5194/tc-7-707-2013> , 2013.

668 Saccò, M., White, N. E., Harrod, C., Salazar, G., Aguilar, P., Cubillos, C. F., ... and  
669 Allentoft, M. E. Salt to conserve: A review on the ecology and preservation of

670 hypersaline ecosystems. *Biol. Rev.*, 96(6), 2828-2850,  
671 <https://doi.org/10.1111/brv.12780> , 2021.

672 Sabbatini, S., Mammarella, I., Arriga, N., Fratini, G., Graf, A., Hörtnagl, L., Ibrom, A.,  
673 Longdoz, B., Mauder, M., Merbold, L., Metzger, S., Montagnani, L., Pitacco, A.,  
674 Rebmann, C., Sedlák, P., Šigut, L., Vitale, D., and Papale, D.: Eddy covariance  
675 raw data processing for CO<sub>2</sub> and energy fluxes calculation at ICOS ecosystem  
676 stations. *Int. Agrophysics.*, 32(4), 495–515, [https://doi.org/10.1515/intag-2017-](https://doi.org/10.1515/intag-2017-0043)  
677 [0043](https://doi.org/10.1515/intag-2017-0043) , 2018.

678 Sharkey, T. D.: Effects of moderate heat stress on photosynthesis: importance of  
679 thylakoid reactions, rubisco deactivation, reactive oxygen species, and  
680 thermotolerance provided by isoprene. *Plant Cell Environ.* 28(3), 269-277,  
681 <https://doi.org/10.1111/j.1365-3040.2005.01324.x> , 2005.

682 Smith, T. P., Thomas, T. J., García-Carreras, B., Sal, S., Yvon-Durocher, G., Bell, T., and  
683 Pawar, S.: Community-level respiration of prokaryotic microbes may rise with  
684 global warming. *Nature comm.*, 10(1), 5124, [https://doi.org/10.1038/s41467-019-](https://doi.org/10.1038/s41467-019-13109-1)  
685 [13109-1](https://doi.org/10.1038/s41467-019-13109-1) , 2019.

686 Song, K. S., Zang, S. Y., Zhao, Y., Li, L., Du, J., Zhang, N. N., ... and Liu, L.:  
687 Spatiotemporal characterization of dissolved carbon for inland waters in semi-  
688 humid/semi-arid region, China. *Hydrol. Earth Syst. Sci.*, 17(10), 4269-4281,  
689 <https://doi.org/10.5194/hess-17-4269-2013> , 2013.

690 Soued, C., Bogard, M. J., Finlay, K., Bortolotti, L. E., Leavitt, P. R., Badiou, P., ... and  
691 Kowal, P.: Salinity causes widespread restriction of methane emissions from small  
692 inland waters. *Nature Comm.*, 15(1), 717, [https://doi.org/10.1038/s41467-024-](https://doi.org/10.1038/s41467-024-44715-3)  
693 [44715-3](https://doi.org/10.1038/s41467-024-44715-3) , 2024.

694 Stoy, P. C., Mauder, M., Foken, T., Marcolla, B., Boegh, E., Ibrom, A., Arain, M. A.,  
695 Arneth, A., Aurela, M., Bernhofer, C., Cescatti, A., Dellwik, E., Duce, P.,  
696 Gianelle, D., van Gorsel, E., Kiely, G., Knohl, A., Margolis, H., Mccaughey, H.,  
697 ... Varlagin, A.: A data-driven analysis of energy balance closure across  
698 FLUXNET research sites: The role of landscape scale heterogeneity. *Agric. For.*  
699 *Meteorol.*, 171–172, 137–152, <https://doi.org/10.1016/j.agrformet.2012.11.004> ,  
700 2013

701 Trenberth, K. E.: Changes in precipitation with climate change. *Clim. Res.* 47(1-2), 123-  
702 138, <https://doi.org/10.3354/cr00953> , 2011.

703 Tweed, S., Grace, M., Leblanc, M., Cartwright, I., and Smithyman, D.: The individual  
704 response of saline lakes to a severe drought. *Sci. Total Environ.*, 409(19), 3919-  
705 3933, <https://doi.org/10.1016/j.scitotenv.2011.06.023> ,2011.

706 Vickers, D., and Mahrt, L.: Quality control and flux sampling problems for tower and  
707 aircraft data. *J. Atmos. Ocean. Techno.*, 14(3), 512–526.,  
708 [https://doi.org/10.1175/1520-0426\(1997\)014<0512:QCAFSP>2.0.CO;2](https://doi.org/10.1175/1520-0426(1997)014<0512:QCAFSP>2.0.CO;2) , 1997.

709 Wang, J., Song, C., Reager, J. T., Yao, F., Famiglietti, J. S., Sheng, Y., ..., and Wada, Y.:  
710 Recent global decline in endorheic basin water storages. *Nature Geosci* 11, 926–  
711 932, <https://doi.org/10.1038/s41561-018-0265-7> , 2018.

712 Webb, E. K., Pearman, G. I., and Leuning, R. Correction of flux measurements for density  
713 effects due to heat and water vapour transfer. *Q. J. R. Meteorol. Soc.* 106 (447),  
714 85–100, <https://doi.org/10.1002/qj.49710644707> ,1980

715 Wen, Z., Song, K., Shang, Y., Fang, C., Li, L., Lv, L., ... and Chen, L.: Carbon dioxide  
716 emissions from lakes and reservoirs of China: a regional estimate based on the  
717 calculated pCO<sub>2</sub>. *Atmos. Environ.*, 170, 71-81,  
718 <https://doi.org/10.1016/j.atmosenv.2017.09.032> , 2017.

719 Williams, W. D.: Environmental threats to salt lakes and the likely status of inland saline  
720 ecosystems in 2025. *Environ. Conserv.*, 29(2), 154-167,  
721 <https://doi.org/10.1017/S0376892902000103> , 2002.

722 Wilson, K., Goldstein, A., Falge, E., Aubinet, M., Baldocchi, D., Berbigier, P., ... &  
723 Verma, S.: Energy balance closure at FLUXNET sites. *Agricultural and Forest*  
724 *Meteorology*, 113(1–4), 223–243, [https://doi.org/10.1016/S0168-1923\(02\)00109-](https://doi.org/10.1016/S0168-1923(02)00109-0)  
725 [0](https://doi.org/10.1016/S0168-1923(02)00109-0) , 2002.

726 Wu, Y., Wang, N., Zhao, L., Zhang, Z., Chen, L. I., Lu, Y., Lü, X., and Chang, J.:  
727 Hydrochemical characteristics and recharge sources of Lake Nuertu in the  
728 Badain Jaran Desert. *Sci. Bull.*, 59(9), 886–895 , [https://doi.org/10.1007/s11434-](https://doi.org/10.1007/s11434-013-0102-8)  
729 [013-0102-8](https://doi.org/10.1007/s11434-013-0102-8) , 2014.

730 Wurtsbaugh, W. A., Miller, C., Null, S. E., DeRose, R. J., Wilcock, P., Hahnenberger,  
731 M., ... and Moore, J.: Decline of the world's saline lakes. *Nat. Geosci.*, 10(11),  
732 816-821, <https://doi.org/10.1038/ngeo3052> , 2017

733 Yan, L., and Zheng, M.: Influence of climate change on saline lakes of the Tibet Plateau,  
734 1973–2010. *Geomorphology*, 246, 68-78,  
735 <https://doi.org/10.1016/j.geomorph.2015.06.006> , 2015.

- 736 Yang, P., Wang, N. A., Zhao, L., Zhang, D., Zhao, H., Niu, Z., and Fan, G.: Variation  
737 characteristics and influencing mechanism of CO<sub>2</sub> flux from lakes in the Badain  
738 Jaran Desert: A case study of Yindeer Lake. *Ecol. Ind.*, 127, 107731,  
739 <https://doi.org/10.1016/j.ecolind.2021.107731> , 2021.
- 740 Yvon-Durocher, G., Caffrey, J. M., Cescatti, A., Dossena, M., Giorgio, P. D., Gasol, J.  
741 M., ... and Allen, A. P.: Reconciling the temperature dependence of respiration  
742 across timescales and ecosystem types. *Nature*, 487(7408), 472-476,  
743 <https://doi.org/10.1038/nature11205> , 2012.
- 744 Yvon-Durocher, G., Jones, J. I., Trimmer, M., Woodward, G. and Montoya, J. M:  
745 Warming alters the metabolic balance of ecosystems. *Phil. Trans. R. Soc. B* 365,  
746 2117–2126, <https://doi.org/10.1098/rstb.2010.0038> , 2010.

## FIGURES

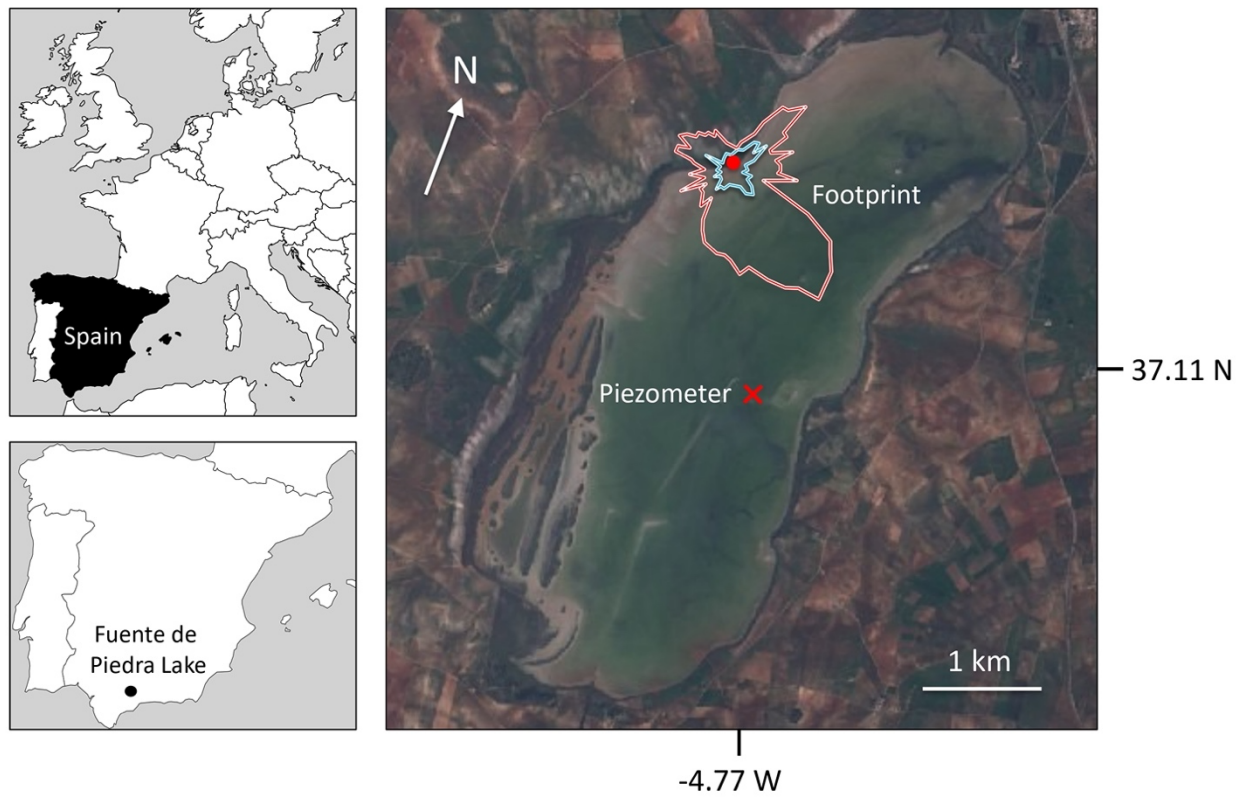


**Fig 1.** Location of the Fuente de Piedra Lake (province of Málaga, South of Spain). Dot inside polygon in right panel shows the location of the eddy covariance tower. The areas within the footprint contributing the 90% to measured fluxes are delimited inside polygons for daytime (blue) and nighttime (red). The cross indicates the location of the piezometer used for measuring groundwater level. Source image: Sentinel-2. Wet image was taken on 17-02-2021.



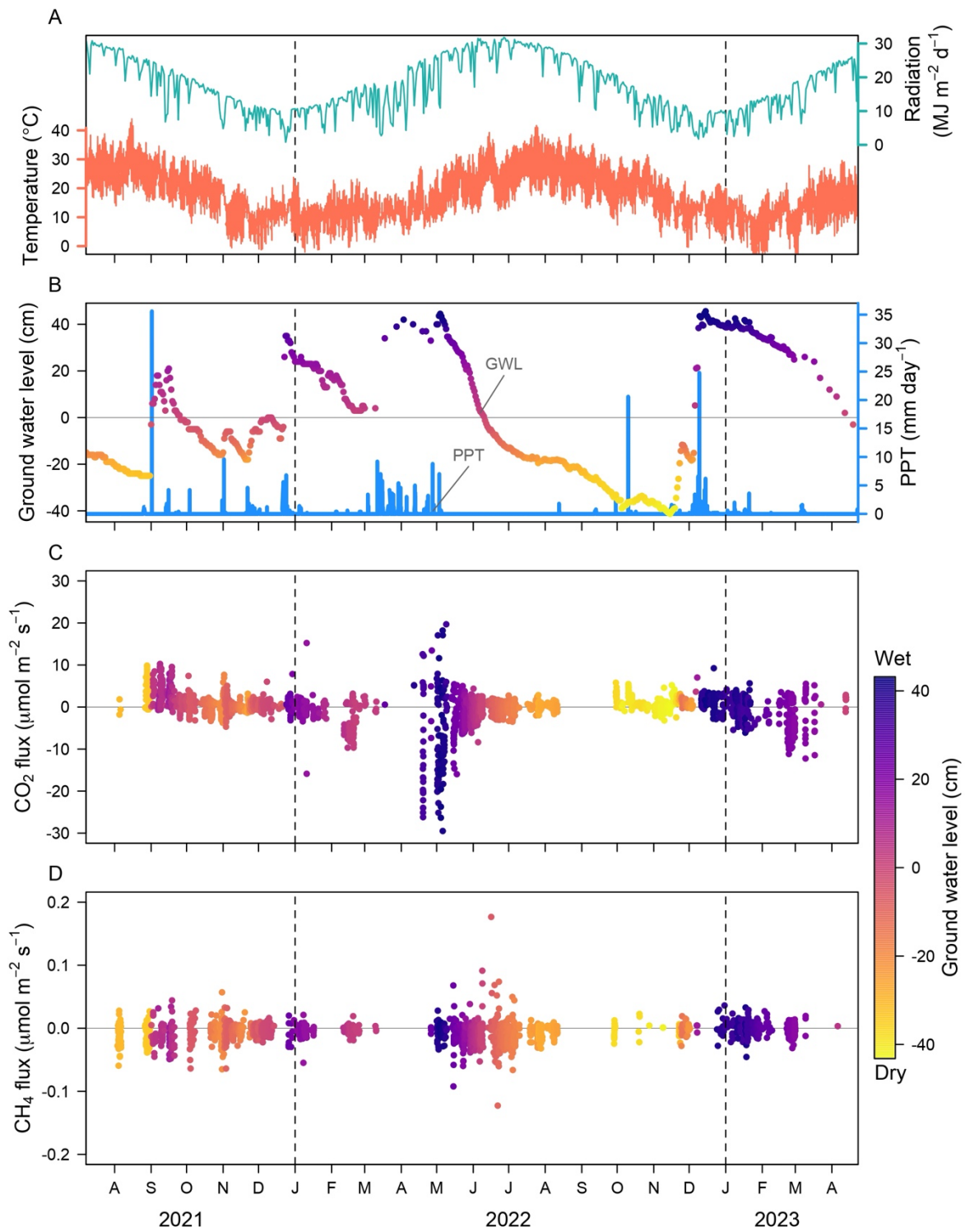


**Fig 2.** Time series of (A) air temperature and incident solar radiation, (B) groundwater level and precipitation (PPT), (C) CO<sub>2</sub> and (D) CH<sub>4</sub> flux, collected at Fuente de Piedra Lake during 2021, 2022, and 2023.

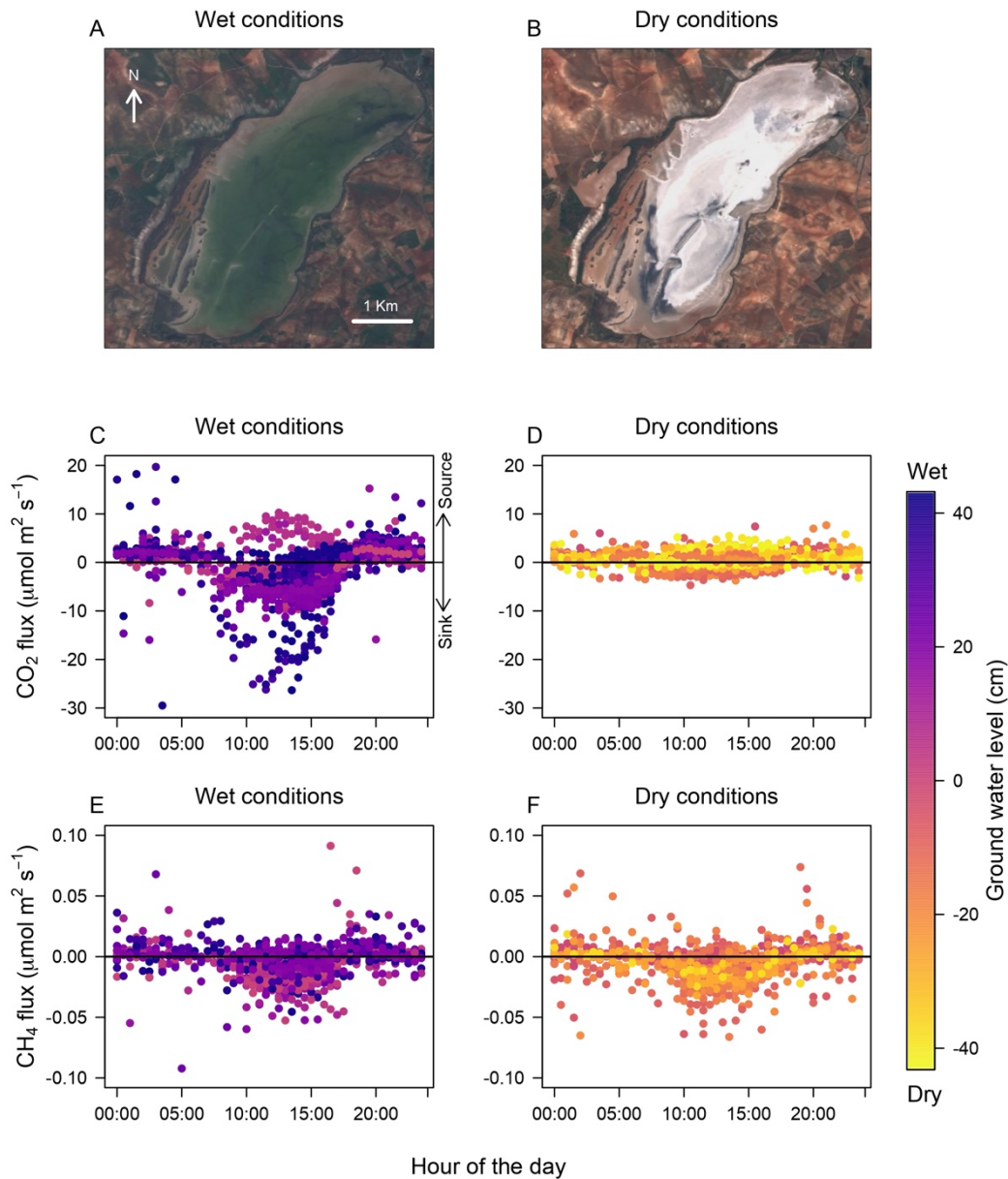


**Fig 3.** Aerial photos of Fuente de Piedra Lake during a period of maximum water availability (wet, **A**) and during a typical dry episode (**B**). Note that for some period during the dry episodes, a salt crust forms covering practically the entire extent of the lake. The figure shows the daily pattern of CO<sub>2</sub> and CH<sub>4</sub> fluxes during wet conditions (**C** and **E** respectively) and dry conditions (**D** and **F** respectively). Water availability is measured in terms of ground water level. Source image: Sentinel-2. Wet image was taken on 17-02-2021 and dry image was taken on 13-5-2021.

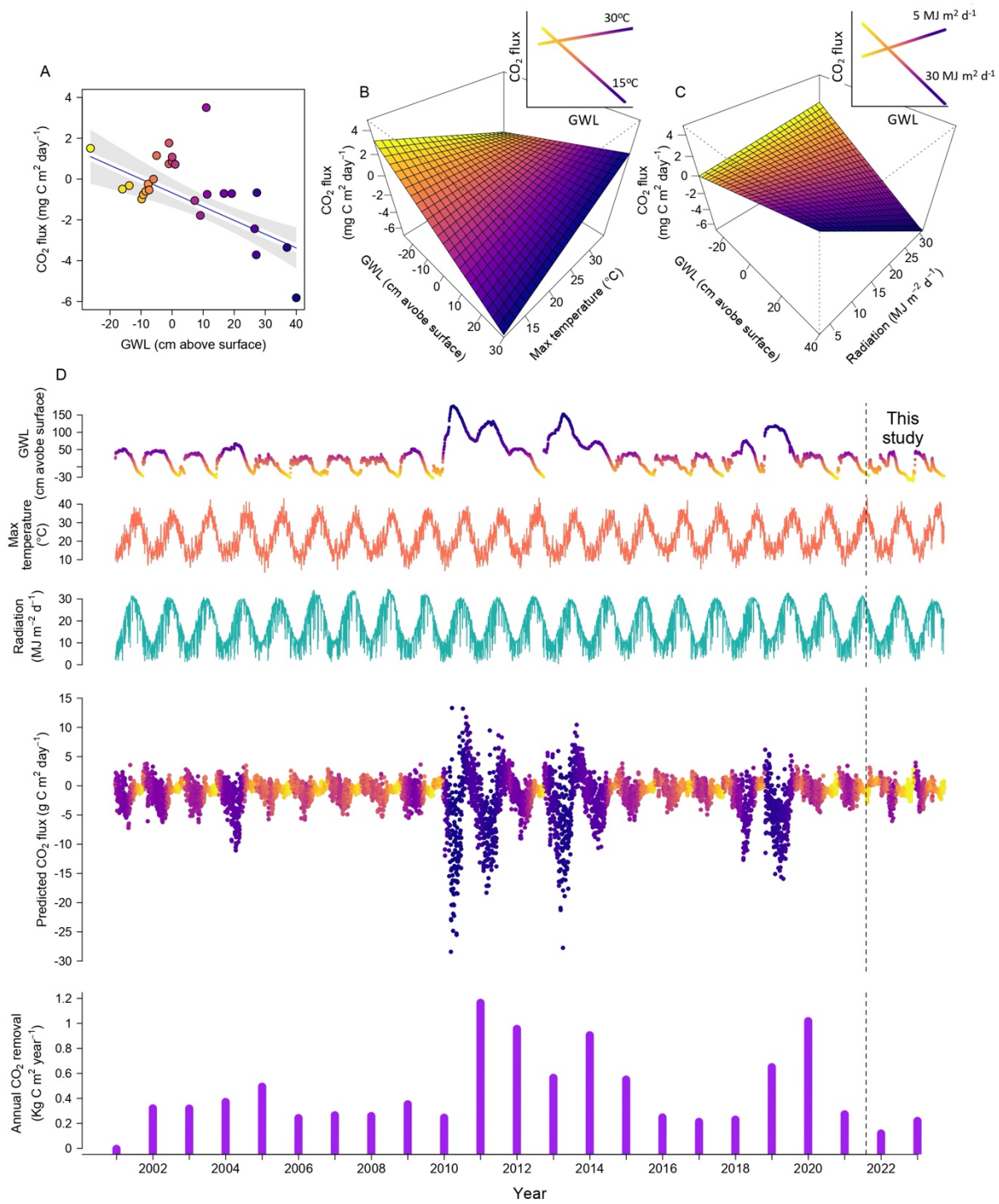


**Fig 4.** Prediction of CO<sub>2</sub> flux as a response to groundwater level with a slope of -0.115 (A), the interaction between groundwater level and daily maximum temperature (B), and the interaction between groundwater level and incident solar radiation (C). Model has an R<sup>2</sup> of 0.73. Using existing time series for the model predictors, it has been possible to reconstruct the estimated CO<sub>2</sub> fluxes, as well as the annual cumulative value of CO<sub>2</sub> removal since 2001 for Fuente de Piedra Lake (D).